

# Cu<sup>II</sup> materials—From crystal chemistry to magnetic model compounds

H. Rosner<sup>a,\*</sup>, M.D. Johannes<sup>b</sup>, S.-L. Drechsler<sup>c</sup>, M. Schmitt<sup>a</sup>, O. Janson<sup>a,d</sup>,  
W. Schnelle<sup>a</sup>, W. Liu<sup>a</sup>, Y.-X. Huang<sup>a</sup>, R. Kniep<sup>a</sup>

<sup>a</sup>Max-Planck-Institut für Chemische Physik fester Stoffe, Nöthnitzer Str. 40, 01187 Dresden, Germany

<sup>b</sup>Naval Research Laboratory, 4555 Overlook Ave., Washington, DC, USA

<sup>c</sup>Institut für Festkörper und Werkstofforschung Dresden, PF 270116, 01171 Dresden, Germany

<sup>d</sup>Department of Crystallography, St. Petersburg State University, Universitetskaya nab. 7/9, 199034 St. Petersburg, Russia

Received 11 May 2007; received in revised form 12 June 2007; accepted 14 June 2007

Available online 22 August 2007

## Abstract

Based on electronic structure calculations within the density functional theory, we report a systematic approach for the modelling of low-dimensional Cu<sup>II</sup> materials. Combining concepts of crystal chemistry with *ab initio*-based magnetic models, we present a systematic study of recently discovered compounds. Our calculation results are in good agreement with thermodynamic and magnetic measurements, suggesting the presented approach as a well-directed route to explore the magnetic phase diagram of low-dimensional Cu<sup>II</sup> systems.

© 2007 NIMS and Elsevier Ltd. All rights reserved.

**Keywords:** Cuprates; Low dimensional; Electronic structure calculation

## 1. Introduction

Low-dimensional spin systems based on transition metal oxides attracted increasing interest in the last few years. This interest was originally triggered by theories of low-dimensional quantum spin models, but more recently this class of compounds, especially Cu<sup>II</sup> materials, became a focus of attention also due to their potential technical applications: promising for optoelectronic applications, ultrafast optical non-linearity was observed [1,2] in the quasi-one-dimensional (1D) compound Sr<sub>2</sub>CuO<sub>3</sub>. Multi-ferroic properties have been discovered lately for the compounds LiVCuO<sub>4</sub> and LiCu<sub>2</sub>O<sub>2</sub> [3,4]. The system Li<sub>2</sub>ZrCuO<sub>4</sub> was found to be close to a quantum critical point [5] and proposed as potential candidate for magnetic cooling applications. Very recently, the Kagomé lattice compounds Cu<sub>3</sub>Zn(OH)<sub>6</sub>Cl<sub>2</sub> and Cu<sub>3</sub>Mg(OH)<sub>6</sub>Cl were discovered [6,7] and are currently being intensely investigated [8,9]; especially with respect to their potential for quantum computational applications [10].

The structural element of Cu(II)-oxygen compounds is the square planar CuO<sub>4</sub> unit, which is shown in Fig. 1 together with the relevant covalent orbitals. The valence electron configuration of Cu<sup>2+</sup> is 3d<sup>9</sup>4s<sup>0</sup>, and that of the O<sup>2-</sup> ion is 2p<sup>6</sup>. The highest occupied atomic orbitals are Cu 3d orbitals and O 2p orbitals. Most of these orbitals are non-bonding. There is one sigma orbital at each ion with the angular dependencies of the wave function given by (x<sup>2</sup>−y<sup>2</sup>)/r<sup>2</sup> for the Cu 3d orbital and by x/r and y/r for the O 2p orbital. The relevant molecular orbital energy level scheme (Fig. 1) shows that the strong covalent d−p bond leads to an energy splitting between the bonding and antibonding levels as large as 10 eV. The fully occupied non-bonding Cu 3d and O 2p levels are in between. Because one electron is missing compared to the fully occupied 3d and 2p shells, the antibonding dp level must be half filled. However, due to a strong intra-atomic correlation present in the Cu 3d orbitals, the molecular field approximation is not sufficient to describe the electronic properties, and the half filled antibonding level splits due to these correlations into a lower and an upper so-called Hubbard level. Thus, these strong correlations are responsible for the insulating behavior of undoped cuprates. According to

\*Corresponding author.

E-mail address: [rosner@cphys.mpg.de](mailto:rosner@cphys.mpg.de) (H. Rosner).

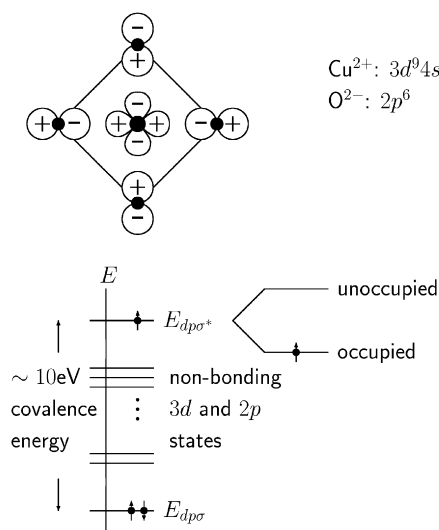


Fig. 1. Top: covalent  $\text{CuO}_4$  square, relevant for the cuprates. The copper ion resides in the center of the square, and the four oxygen ions occupy the corners. The antibonding molecular orbital is shown with sign changes of the wave function on all four Cu–O bonds, so that the wave function has nodes on the bonds. Bottom: molecular orbital scheme of the covalent  $\text{CuO}_4$  square; the half-filled antibonding level is split due to strong on-site Coulomb correlations.

the occupation of the molecular levels shown in Fig. 1, the  $\text{CuO}_4$  unit is magnetically active, carrying a spin 1/2. Owing to this small and localized moment, compounds with  $\text{CuO}_4$  units are ideal objects to study the effect of quantum fluctuations.

General interest in magnetically low-dimensional systems began with the advent of quantum mechanics and the development of spin–spin interaction models in order to explain the magnetic behavior. Although deceptively simple, early models such as Ising and Heisenberg models have exact ground state solutions only in one or two dimensions (2D), respectively, or no such solution is known. The search for real materials with substantially 1D or 2D magnetic interactions initially had the purpose of verifying or disproving theoretical predictions of exotic ground states associated with strong quantum fluctuation effects [11]. Later, a more practical aspect came to light when quantum spin fluctuations were suggested as possible mediators for unconventional pairing in some superconductors, most notably in the quasi-2D high-temperature cuprates [12].

The architecture of quasi-planar structures by linking  $\text{CuO}_4$  squares that share one or two common oxygen positions was first considered by Müller-Buschbaum [13] on an empirical basis (long before the high- $T_c$  cuprate superconductors were discovered). Composing the basic  $\text{CuO}_4$  units like bricks from a toy box leads to more and more complex networks [14] with an intriguing variety of magnetic ground states. A few possible arrangements are sketched in Fig. 2. Isolated  $\text{CuO}_4$  squares (Fig. 2a) can be present in connection with complex anions such as sulfate or phosphate groups like in the crystal structures of

$\text{CuPbSO}_4(\text{OH})_2$  and  $\text{Sr}_2\text{Cu}(\text{PO}_4)_2$  [16], respectively. In other compounds  $\text{CuO}_4$  squares may share common oxygen positions forming structural arrangements as sketched in Fig. 2b–d. Depending on the number of shared oxygen atoms, they can form corner-sharing chains (see Fig. 2b), edge-sharing chains (Fig. 2c) or double chains (Fig. 2d). By a combination of the chains, a rich variety of two-, three- or multi-leg ladders can be built [15]. In this way, a quasi-continuous transition is possible from 1D to 2D Cu(II) compounds. Thus, a better understanding of the electronic and magnetic properties of quasi-1D chain compounds can be a key for a deeper understanding of the high-temperature oxide-superconductors.

## 2. Electronic structure calculations

To extract the main ingredients for the electronic and magnetic properties of real compounds, density functional (DFT) calculations are a valuable tool. From the calculated electronic structure, the involved orbitals and the leading interactions can be estimated in terms of a tight-binding (TB) model. Subsequently, such a TB model can be mapped to an extended Hubbard or Heisenberg model to improve the description of the above-mentioned strong intra-atomic correlations at the Cu sites. From the approximate solution of such models, the magnetic ground state and its excitations can be estimated. In the following, this procedure is demonstrated exemplarily for the compounds  $\text{Sr}_2\text{Cu}(\text{PO}_4)_2$  [16] and  $\text{ACu}_2\text{O}_2$  ( $A = \text{Na}, \text{Li}$ ) [17–21].

$\text{Sr}_2\text{Cu}(\text{PO}_4)_2$  and the isotopic  $\text{Ba}_2\text{Cu}(\text{PO}_4)_2$  exhibit a structural arrangement which is unique among known quasi-1D chains (see Fig. 3): planar  $\text{CuO}_4$  squares are isolated from each another and are linked by  $\text{PO}_4$  tetrahedra to form infinite chains. Nearest neighbor squares are coplanar and run along [0 1 0] which represents the chain direction.  $\text{CuO}_4$  squares of adjacent chains (along [1 0 0]) occupy the positions “between” the squares of neighboring chains on both sides. Along [0 0 1] adjacent chains are separated by the full length of the unit cell parameter. Taking into account the structural details of  $\text{Sr}_2\text{Cu}(\text{PO}_4)_2$  the compound would be best described as phosphato-cuprate (II) with the anionic partial structure given by  $[\text{Cu}(\text{PO}_4)_2]^{4-}$ .

Band structure calculations have been carried out within the local density approximation (LDA) using the full-potential local orbital code, FPLO [22]. The paramagnetic band structure of  $\text{Sr}_2[\text{Cu}(\text{PO}_4)_2]$  (Fig. 4) shows a single half-filled band, derived from the Cu  $3d_{x^2-y^2}$  orbital, crossing the Fermi energy. Only the inclusion of strong electron correlations leads to the insulating behavior which is experimentally observed. The 1D character of the system is qualitatively obvious from the nearly dispersionless bands in directions  $S$ – $Y$  and  $\Gamma$ – $Z$  which are perpendicular to the chain direction, and from the characteristic logarithmic divergences in the density of states (DOS) near the band edges (Fig. 4 inset). To compare quantitatively

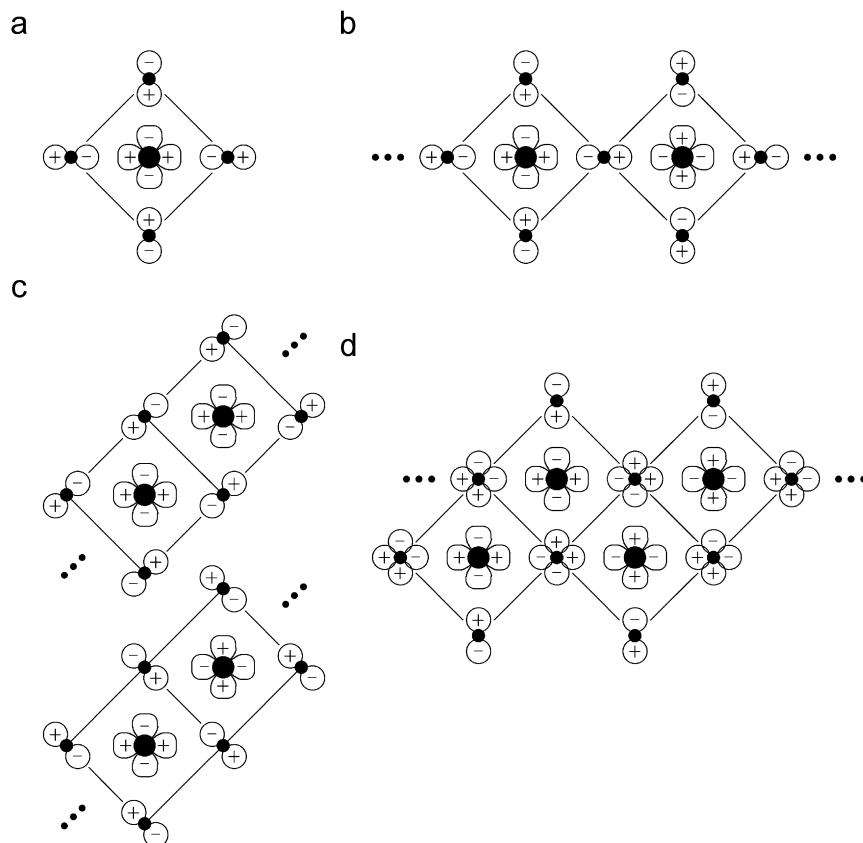


Fig. 2. Cuprate chains formed from the square (a) as the building block. A corner-sharing chain (b), an edge-sharing chain (c), and a double chain (d) are shown. The phase factors of the orbitals correspond to the antibonding state.

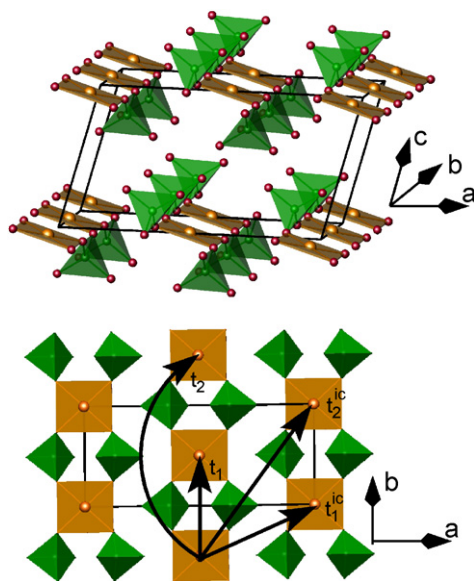


Fig. 3. Top: crystal structure of  $\text{Sr}_2[\text{Cu}(\text{PO}_4)_2]$  showing the isolated  $\text{CuO}_4$  squares from which the Heisenberg spin chains are formed. Bottom: a top view of the spin chain plane with the various electronic hopping paths labelled. Hopping in the out-of-page direction is not shown.

microscopic magnetic interactions, we fitted a TB model to our band structure and calculated the individual exchange constants between various Cu spins using  $J_{ij} = 4t_{ij}^2/U$  with a standard  $U = 4.5$  eV. The hopping parameters included

in the model are shown schematically in Fig. 3 (bottom). The resulting TB dispersion is indistinguishable from the full-potential calculation (Fig. 4 top), indicating that further interactions can be safely ignored. The ratio of the strongest in-plane coupling to the strongest inter-chain coupling is  $J_1/J_1^c \sim 70$  and the ratio of first to second neighbor in-chain coupling is  $J_1/J_2 \sim 700$  for  $\text{Sr}_2\text{Cu}(\text{PO}_4)_2$ . Identical calculations based on the band structure of  $\text{Ba}_2[\text{Cu}(\text{PO}_4)_2]$  (not shown) yield similar results with slightly more inter-chain coupling but less second neighbor in-chain coupling. Both systems can therefore be considered as strongly 1D, with  $\text{Ba}_2[\text{Cu}(\text{PO}_4)_2]$  slightly less so. These results are confirmed by additional LSDA + U calculations.

The 1D nature of magnetic interactions in  $\text{Sr}_2[\text{Cu}(\text{PO}_4)_2]$  can be traced back to the isolated  $\text{CuO}_4$  squares. This construction virtually eliminates the second neighbor in-chain coupling that prevents compounds such as  $\text{Li}_2\text{CuO}_2$  from being described via a simple nearest neighbor Heisenberg model [23,24]. Cuprates such as  $\text{Sr}_2\text{CuO}_3$  containing corner-sharing  $\text{CuO}_4$  squares have by far smaller second neighbor interactions, of the order  $J_1/J_2 \sim 15$ , and yet, these must be taken into account to get good agreement between model calculations and experiment [25]. Conceptualized in this way, one can make a correspondence between exchange constants in edge-sharing  $\text{CuO}_4$  systems (es) and those with isolated  $\text{CuO}_4$  squares (i):  $J_2^{\text{es}} \rightarrow J_1^{\text{i}}$  and  $J_4^{\text{es}} \rightarrow J_2^{\text{i}}$ . Since  $J_4^{\text{es}}$  is known to be vanishingly small, it is clear that the second

neighbor interactions between isolated squares can be expected to be negligible. New experimental results confirm an extraordinary one dimensionality with no long-range-order above the mK temperature range. Low-temperature thermodynamic measurements down to 30 mK show long-range order only below  $T_N = 0.085$  K [26]. This temperature is about 2000 times smaller than the leading interaction  $J_1$  along the chain, showing that quantum fluctuations dominate the low-temperature magnetic properties of this system.

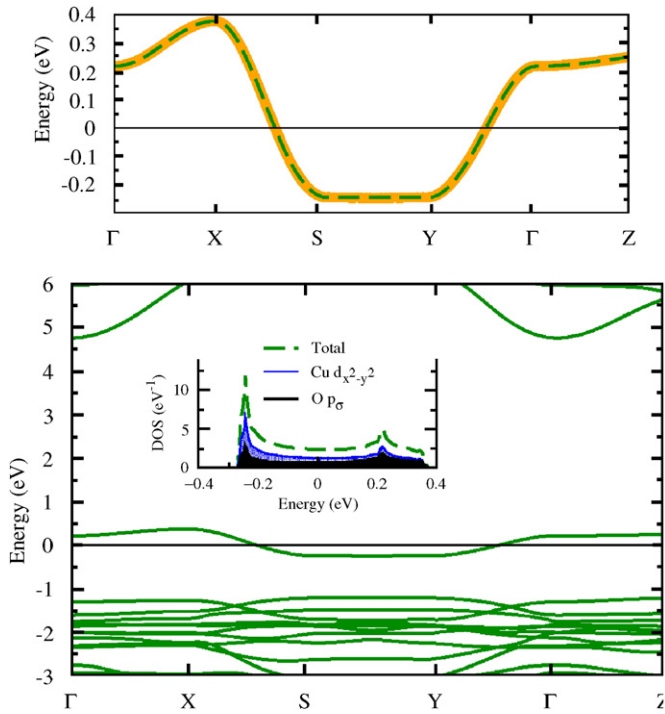


Fig. 4. Band structure of  $\text{Sr}_2[\text{Cu}(\text{PO}_4)_2]$ , showing the single metallic band well separated from all others. The  $X$ - $S$  direction is along the magnetic chain,  $S$ - $Y$  and  $\Gamma$ - $Z$  directions are perpendicular to the chain. In the top panel, a blow-up of this band is shown with TB eigenvalues superimposed to show the remarkable reproduction of the dispersion. The inset shows the total and orbitally resolved DOS for the single band.

We have shown that the isolated  $\text{CuO}_4$  squares in  $\text{Sr}_2[\text{Cu}(\text{PO}_4)_2]$  allow for an excellent description of its magnetic and thermodynamic properties using a 1D nearest-neighbor-only Heisenberg spin- $\frac{1}{2}$  model. We calculated the exchange constant and extracted it from experimental data and found extremely good agreement between the two.  $\text{Sr}_2[\text{Cu}(\text{PO}_4)_2]$  is the best realization for the 1D nearest neighbor Heisenberg model so far. We anticipate that  $\text{Sr}_2[\text{Cu}(\text{PO}_4)_2]$  will be useful as a real physical system that can be compared with theoretical models with confidence that deviations from prediction are due to actual effects beyond the Heisenberg Hamiltonian rather than to non-1D or distant neighbor interactions.

Another example for the realization of an unusual magnetic ground state is the isostructural compounds  $\text{LiCu}_2\text{O}_2$  and  $\text{NaCu}_2\text{O}_2$ , which exhibit a helical magnetic order at low temperatures [17–21]. The crystal structure of  $\text{LiCu}_2\text{O}_2$  and  $\text{NaCu}_2\text{O}_2$  is shown in Fig. 5 and consists of bilayers of edge-sharing  $\text{Cu}^{\text{II}}\text{O}_{4/2}$  chains that run along the crystallographic  $b$ -axis. The  $\text{Cu}^{\text{II}}\text{O}_{4/2}$  chains are linked by non-magnetic  $\text{Cu}^{\text{I}}\text{O}$  dumbbells, thus forming the bilayer. Similarly to  $\text{Sr}_2[\text{Cu}(\text{PO}_4)_2]$ , we mapped the LDA band structure (not shown) of this system to a TB model, shown in the right panel of Fig. 5. In contrast to  $\text{Sr}_2[\text{Cu}(\text{PO}_4)_2]$ , we find dominating second neighbor interactions and a considerable inter-chain coupling. Including the ferromagnetic component of the nearest neighbor exchange  $J_1$  arising from the almost  $90^\circ$   $\text{Cu}^{\text{II}}\text{O}-\text{Cu}^{\text{II}}$  bond angle along the chains, we end up with competing magnetic interactions along the  $\text{Cu}^{\text{II}}\text{O}_{4/2}$  chain: ferromagnetic  $J_1 \sim -50$  K and antiferromagnetic  $J_2 \sim 100$  K. This competition leads to strong magnetic frustration and, as predicted from model calculations, to a helimagnetic order along the chains in agreement with the experimental observations.

Recently, we investigated the magnetic properties of  $\text{Cu}_2[\text{PO}_6(\text{CH}_2)]$  [27]. From the structural point of view, this compound is situated in “between” the systems discussed above. It consists of isolated dimers ( $\text{O}_2\text{CuO}_2\text{CuO}_2$ ), formed by two  $\text{CuO}_4$  units sharing a common edge. The

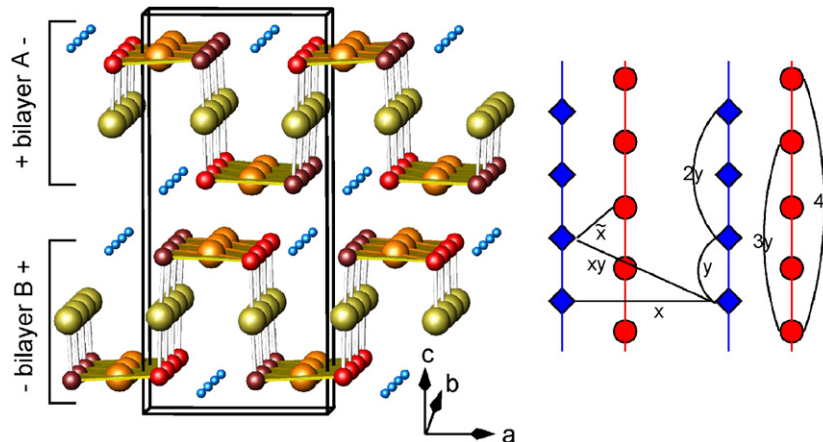


Fig. 5. (Left) Crystal structure of  $\text{ACu}_2\text{O}_2$  ( $A = \text{Na}, \text{Li}$ ) with two bilayers of  $\text{CuO}_2$  chains running along  $b$  ( $\text{Cu}^{2+}$  orange,  $\text{Cu}^{1+}$  yellow, inner (outer) O red (brown), Na blue). (Right) Schematic chain structure with the main exchange paths indicated. Filled diamonds and circles denote  $\text{CuO}_2$  squares in A and B bilayers, respectively.

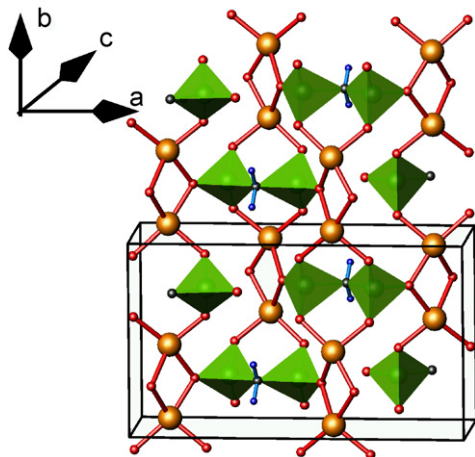


Fig. 6. Crystal structure of  $\text{CuPO}_6(\text{CH}_2)$ . The  $\text{CuO}_4$  units form distorted dimers along the  $b$  direction. They are linked by  $\text{O}_3\text{PCH}_2\text{PO}_3$  groups (green) similar to pyrophosphate groups  $\text{P}_2\text{O}_7$ .

long axes of the dimers are arranged in direction of the crystallographic  $b$ -axis (see Fig. 6). The dimers are distorted significantly and connected via  $\text{O}_3\text{P}(\text{CH}_2)\text{PO}_3$ -groups. First experimental and theoretical results indicate that this compound exhibits a spin gap at low temperatures. According to a TB model and supported by LSDA+U total energy calculations, the compound can be described best by an alternating chain model. The magnetic exchange within the structural dimers and between them along the  $b$ -axis are antiferromagnetic and of comparable size, causing a narrow spin gap. In addition, we find sizeable antiferromagnetic inter-dimer couplings perpendicular to the dimer chains. These interactions have strongly frustrating character, enhancing the spin gap further. To clarify the nature of the magnetic coupling and the exact mechanism for the spin gap formation, further investigations on single crystals are required.

### 3. Summary and outlook

We have shown that the magnetic properties of low-dimensional  $\text{Cu}^{\text{II}}$  compounds strongly depend on details of their crystal structures such as bond angles and lengths. Microscopic magnetic models based on DFT electronic structure calculation offer the possibility to connect these structural aspects with the magnetic properties in a quantitative way. Using complex oxo-anions of non-metals (e.g. B,C,P,S...) as space- and direction-controlling agents for  $\text{Cu}^{\text{II}}$  coordination squares (and their interconnections), a large variety of compounds with intriguing magnetic properties could be constructed and prepared. Thus, we expect that the combination of theoretical electronic structure calculations, thermodynamic and spectroscopic investigations together with well-directed crystal chemical aspects will be a powerful tool for future exploration of quantum phase diagrams of low-dimensional materials.

### Acknowledgments

Financial support of the Emmy-Noether-Programm of the Deutsche Forschungsgemeinschaft and of the German-Israeli Foundation (Grant 811-237.14103) is acknowledged. We thank the ZIH Dresden for the use of their computational facilities.

### References

- [1] T. Ogasarawa, M. Ashida, N. Motoyama, H. Eisaki, S. Uchida, Y. Tokura, H. Ghosh, A. Shukla, S. Mazumdar, M. Kuwata-Gonokami, *Phys. Rev. Lett.* 85 (2000) 2204.
- [2] H. Kishida, M. Ono, K. Miura, H. Okamoto, M. Izumi, T. Manako, M. Kawasaki, Y. Taguchi, T. Tohyama, K. Tsutsui, S. Maekawa, *Phys. Rev. Lett.* 87 (2001) 177401.
- [3] Y. Naito, K. Sato, Y. Yasui, Yu. Kobayashi, Yo. Kobayashi, M. Sato, *J. Phys. Soc. Jpn.* 76 (2007) 023708.
- [4] S. Park, Y.J. Choi, C.L. Zhang, S.-W. Cheong, *Phys. Rev. Lett.* 98 (2007) 057601.
- [5] S.-L. Drechsler, O. Volkova, A.N. Vasiliev, N. Tristan, J. Richter, M. Schmitt, H. Rosner, J. Malek, R. Klingeler, A.A. Zvyagin, B. Büchner, *Phys. Rev. Lett.* 98 (2007) 175203.
- [6] W. Krause, H.-J. Bernhardt, R.S.W. Braithwaite, U. Kilitsch, R. Pritchard, *Mineral. Mag.* 70 (2007) 329.
- [7] T. Malcherek, J. Schlüter, *Acta Crystallogr. B* 63 (2007) 157.
- [8] J.S. Helton, K. Matan, M.P. Shores, E.A. Nylko, B.M. Barlett, Y. Yoshida, Y. Takano, A. Suslov, Y. Qiu, J.-H. Chung, D.G. Nocera, S. Lee, *Phys. Rev. Lett.* 98 (2007) 107204.
- [9] G. Misguich, P. Sindzingre, *Cond-Mat*, 0704-1017.
- [10] B.G. Levi, *Phys. Today* 60 (2007) 16.
- [11] U. Schollwöck, J. Richter, D.J.J. Farnell, R.F. Bishop (Eds.), *Quantum Magnetism, Lecture Notes in Physics*, vol. 645, Springer, Berlin, 2004.
- [12] J.P. Carbotte, E. Schachinger, N.D. Basov, *Nature* 401 (1999) 354.
- [13] H. Müller-Buschbaum, *Angew. Chem.* 89 (1977) 704.
- [14] L. Leonyuk, V. Maltsev, G.-J. Babonas, R. Szymczak, H. Szymczak, M. Baranc, *Acta Crystallogr. A* 57 (2001) 34.
- [15] E. Dagotto, T.M. Rice, *Science* 271 (1996) 618.
- [16] M.D. Johannes, J. Richter, S.-L. Drechsler, H. Rosner, *Phys. Rev. B* 74 (2006) 174435.
- [17] T. Masuda, A. Zheludev, A. Bush, M. Markina, A. Vasiliev, *Phys. Rev. Lett.* 92 (2004) 77201.
- [18] A.A. Gippius, E.N. Morozova, A.S. Moskvin, A.V. Zalessky, A.A. Bush, M. Baenitz, H. Rosner, S.-L. Drechsler, *Phys. Rev. B* 70 (2004) 020406.
- [19] S.-L. Drechsler, J. Málek, J. Richter, A.S. Moskvin, A.A. Gippius, H. Rosner, *Phys. Rev. Lett.* 94 (2005) 039705.
- [20] L. Capogna, M. Mayr, P. Horsch, M. Raichle, R.K. Kremer, M. Sonin, B. Keimer, *Phys. Rev. B* 71 (2005) 140402.
- [21] S.-L. Drechsler, J. Richter, A.A. Gippius, A. Vasiliev, A.A. Bush, A.S. Moskvin, J. Málek, Y. Prots, W. Schnelle, H. Rosner, *Europhys. Lett.* 73 (2006) 83.
- [22] K. Koepernik, H. Eschrig, *Phys. Rev. B* 59 (1999) 1743.
- [23] R. Weht, W.E. Pickett, *Phys. Rev. Lett.* 81 (1998) 2502.
- [24] R. Neudert, H. Rosner, S.-L. Drechsler, M. Kielwein, M. Sing, M. Knupfer, M.S. Golden, J. Fink, N. Nücker, S. Schuppler, N. Motoyama, H. Eisaki, S. Uchida, Z. Hu, M. Domke, G. Kaindl, *Phys. Rev. B* 60 (1999) 13413.
- [25] H. Rosner, H. Eschrig, R. Hayn, S.-L. Drechsler, J. Malek, *Phys. Rev. B* 56 (1997) 3412.
- [26] A.A. Belik, S. Uji, T. Terashima, E. Takayama-Muromachi, *J. Solid State Chem.* 178 (2005) 3461.
- [27] H. Rosner, M. Schmitt, W. Schnelle, A. Gippius, W. Liu, Y. Huang, R. Kniep, to be published.